

# An innovative technique for pore structure analysis of fuel cell and battery components using flow porometry

Akshaya Jena, Krishna Gupta\*

*Porous Materials, Inc., 83 Brown Road, Ithaca, NY 14850, USA*

Received 30 November 2000; accepted 10 December 2000

## Abstract

Some of the porous sheet materials used in fuel cells and batteries hardly permit gas flow through the thickness of the sheet, although flow parallel to the sheet is appreciable. Determination of the porosity of such materials is not possible by the available techniques. A novel technique based on flow porometry is reported. This technique can measure the pore structure of such porous sheets. A composite porous sheet material containing one of the electrodes and the separator in two layers was investigated. The largest pore diameter, the mean flow pore diameter and the pore size distributions were measured. The pore structures of both layers were identified. © 2001 Elsevier Science B.V. All rights reserved.

*Keywords:* Capillary flow porometry; Pore structure; Fuel cell separators; Battery separators

## 1. Introduction

Recent research efforts to design more efficient batteries and fuel cells have resulted in the development of thin composite sheets of porous materials. Composites of electrode and separator materials and composite separators are examples of such porous sheets. These sheet materials often hardly permit gas flow through the thickness of the sheet, although flow parallel to the sheet is appreciable. Porosity of such composite materials is vital for design applications. However, determination of the pore structure of such materials is not possible by the available techniques. The widely used mercury intrusion technique and the vapor condensation technique cannot be employed because the pore volume in the thin sheet is too small to be detectable. Flow porometry measures flow rate parallel to the thickness of the sheet. This technique cannot measure the pore structures of composites consisting of several layers.

In order to measure the pore structure of composite porous sheets, a novel technique based on flow porometry has been designed. In this paper the new technique is described and results obtained with a two layered composite battery material are discussed.

## 2. Material and techniques

### 2.1. Material

A composite sheet material consisting of an electrode and the separator was investigated. The two layers had different pore sizes. Fig. 1 is an illustration of the structure of the material. The pore size in layer no. 1 is much smaller than the pore size in layer no. 2.

### 2.2. Principle of the technique

The sample of the material to be tested is soaked in a liquid that fills spontaneously the pores in the material. The liquid is known as the wetting liquid. Filling of the pores by the liquid results in replacement of the solid/gas interface by a solid/liquid interface. Spontaneous filling occurs because the interfacial free energy of the solid/liquid interface is lower than that of the solid/gas interface and the net free energy change associated with the filling process is negative. Removal of the wetting liquid from pores is not spontaneous. Therefore, pressure of a non-reacting gas is slowly increased on one side of the sample to remove the liquid from pores and permit gas flow to occur.

Gas displaces the liquid in the pore, when work done by the gas is equal to the increase in surface free energy (Fig. 2).

\* Corresponding author. Tel.: +1-607-257-5544; fax: +1-607-257-5639.  
E-mail address: info@pmiapp.com (K. Gupta).

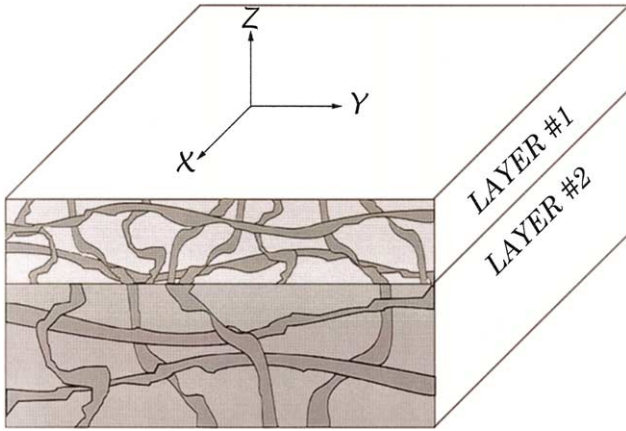


Fig. 1. The two layered battery material.

Considering displacement of a small volume of liquid

$$p dV = \gamma_{s/g} dS_{s/g} + \gamma_{s/l} dS_{s/l} + \gamma_{l/g} dS_{l/g} \quad (1)$$

Where,  $p$  is the differential pressure;  $V$  the volume of gas in the pore;  $\gamma_{s/g}$  the solid/gas interfacial free energy;  $S_{s/g}$  the solid/gas surface area;  $\gamma_{s/l}$  the solid/liquid interfacial free energy;  $S_{s/l}$  the solid/liquid interfacial area;  $\gamma_{l/g}$  the liquid/gas interfacial free energy;  $S_{l/g}$  the liquid/gas interfacial area.

Increase in solid/gas surface area is equal to the decrease in the solid/liquid surface area.

$$dS_{s/g} = -dS_{s/l} \quad (2)$$

Substituting in Eq. (1)

$$p = \gamma_{l/g} \left( \frac{dS_{s/g}}{dV} \right) \left\{ \left[ \frac{\gamma_{s/g} - \gamma_{s/l}}{\gamma_{l/g}} \right] + \left[ \frac{dS_{l/g}}{dS_{s/g}} \right] \right\} \quad (3)$$

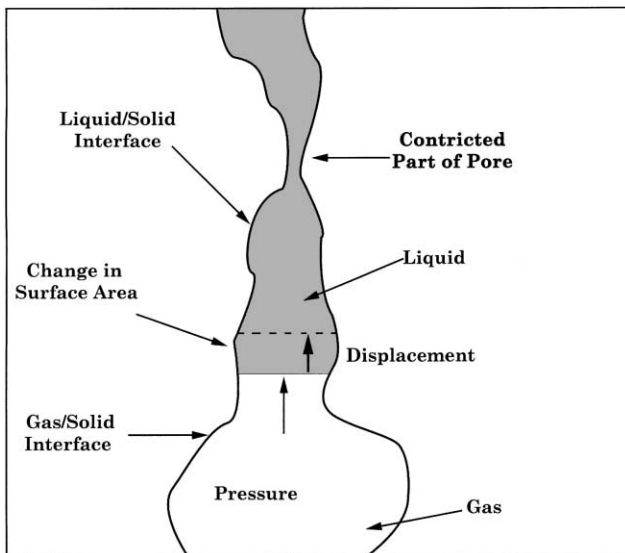


Fig. 2. Displacement of liquid in the pore by gas.

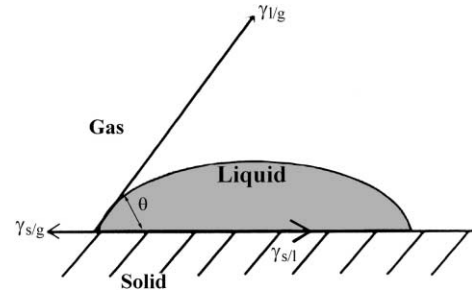


Fig. 3. Equilibrium between the three surface tensions.

In the case of consolidated materials and high fiber density materials the term,  $[dS_{l/g}/dS_{s/g}]$  is very small.

$$\left[ \frac{dS_{l/g}}{dS_{s/g}} \right] \approx 0 \quad (4)$$

The surface tensions can be expressed in terms of contact angle,  $\theta$ , of the wetting liquid with the solid. Equilibrium between the surface tensions depicted in Fig. 3 shows that

$$\cos \theta = \left[ \frac{\gamma_{s/g} - \gamma_{s/l}}{\gamma_{l/g}} \right] \quad (5)$$

It has been demonstrated that for wetting liquids with very low surface tensions [1]:

$$\cos \theta \approx 1 \quad (6)$$

Substituting from relations 4, 5 and 6 in Eq. (3)

$$p = \gamma_{l/g} \left( \frac{dS_{s/g}}{dV} \right) \quad (7)$$

It follows from this relation that the lowest pressure is required to empty the largest pore (lowest  $[dS/dV]$ ). Therefore, there will be no flow through the sample containing liquid filled pores and flow of gas begins when the pressure is increased to a value sufficient to empty the largest pore. Further increase of pressure will empty smaller pores and increase gas flow. Measurement of flow rate as a function of differential pressure permits many pore characteristics to be measured.

### 2.3. The instrument

In order to obtain reliable and reproducible results, the instrument was fully automated and contained many novel design features and state-of-the-art components. Windows-based operation of the instrument made testing objective easy. The instrument is shown in Fig. 4.

The unique design of the sample chamber shown in Fig. 5 allows gas flow to occur only along the  $x$  and  $y$  directions (Fig. 1). We call this flow parallel to the plane of the sheet in-plane flow. The wet sample is placed between two non-porous plates. The bottom plate has a small central opening.



Fig. 4. Capillary flow porometer.

Compressed gas reaches the wet sample through the central hole. Gas is permitted to pass through the  $x$  and  $y$  directions in the plane of the sheet material. Differential pressure and flow rate in the in-plane directions are measured.

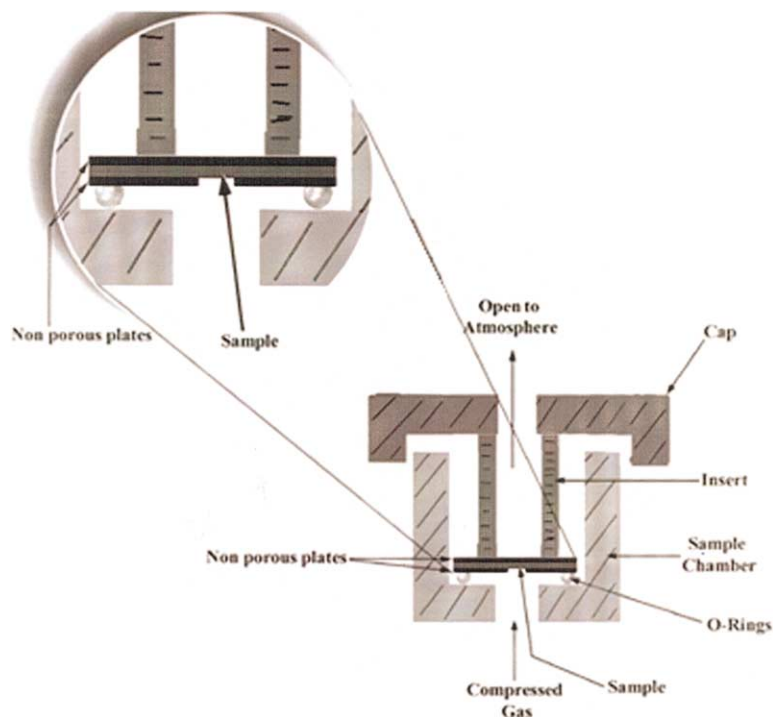


Fig. 5. Sample chamber for determination of in-plane pore structure.

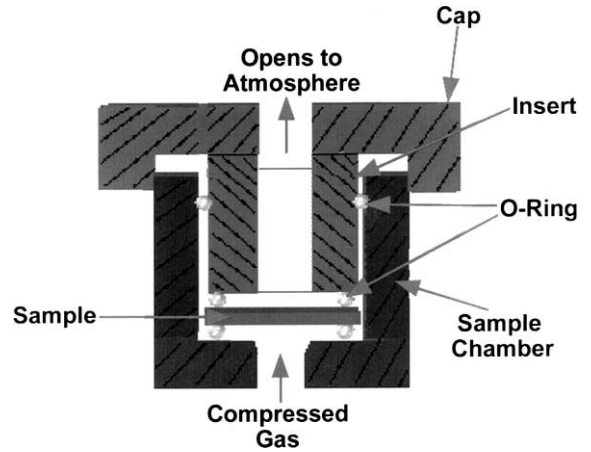


Fig. 6. Sample chamber for determination of through-plane pore structure.

The sample chamber shown in Fig. 6 allows gas to flow only along the  $z$  direction (Fig. 1). We call this through plane flow. The in-plane flow is prevented by O-rings. The differential pressure and through-plane flow rates are measured.

### 3. Results and discussion

#### 3.1. Variation of flow rate with differential pressure

Fig. 7 shows the variation of flow rate with differential pressure when the sample chamber for flow along the  $z$  direction (through-plane) was used (Fig. 6). The data are

presented as three curves. The dry and wet curves are obtained with dry (liquid free) and wet (liquid filled) samples, respectively. The half-dry curve is calculated from the dry curve and yields half of the flow rate through the dry sample at any given pressure.

All the pores in the dry sample are open. Therefore, the flow continuously increases with increase of pressure. The pores in the wet sample are filled with liquid. Therefore, there is no flow at the start. When the pressure is sufficient to empty the largest pore, flow starts and on further increase of pressure flow rate increases.

Gas pressure required to displace the liquid in the pore and start flow through the pore is determined by pore size. The size of a pore varies along its length (Fig. 2) and the gas pressure required to displace the liquid also varies along the length of the pore. The pressure is maximum at the most constricted part of the pore because  $(dS/dV)$  of the pore has its maximum value at this part. Only when the pressure reaches this maximum, is the liquid in the pore completely removed and gas flows through the pore. Thus, measured pressure for flow to occur through a pore corresponds to the size of the narrowest part of the pore. For through-plane flow, the layers in the sample are in series and the pores extend from layer no. 2 to layer no. 1. Therefore, the measured differential pressure is due to the size of the smaller pores in layer no. 1.

Fig. 7 also contains data from the specimen loaded in the sample chamber (Fig. 5) which permitted flow in the  $x$  and  $y$  directions (in-plane). The layers in the sample are parallel and gas could flow in the  $x$  and  $y$  directions in both layers simultaneously. However, the pores in layer no. 2 are larger than the pores in layer no. 1. Therefore, the pores in layer no.

2 require less pressure to be emptied. In-plane flow at low pressures occurs through the large pores in layer no. 2 and when the pressure is sufficiently high flow also occurs through the small pores in layer no. 1. Therefore, the in-plane flow rate is expected to be much larger than the through-plane flow rate. This is observed in Fig. 7.

### 3.2. Pore diameter

Pore cross-sections are normally irregular. Therefore, pore size is not defined. We define pore diameter as the diameter,  $D$  of an opening such that:

$$\left(\frac{dS}{dV}\right)_{\text{pore}} = \left(\frac{dS}{dV}\right)_{\text{opening}} = \frac{4}{D} \quad (8)$$

Substituting in Eq. (7)

$$D = \frac{4\gamma_{l/g}}{p} \quad (9)$$

Eq. (9) is used to calculate pore diameter.

The largest pore diameter is obtained from the pressure at which the flow of gas begins. This pressure is known as the bubble point pressure. The instrument uses a sophisticated technique to detect this pressure accurately. The largest pore diameters were calculated after Eq. (9) using the measured bubble point pressures and surface tension of the wetting liquid. The results are listed in Table 1. The largest pore diameter obtained by in-plane flow is for layer no. 2 and the one obtained by through-plane flow is for layer no. 1. As expected, the largest pore diameter in layer no. 1 is much smaller (about one fifth) than that in layer no. 2. The ability of the separator to act as a barrier to certain ions and particles

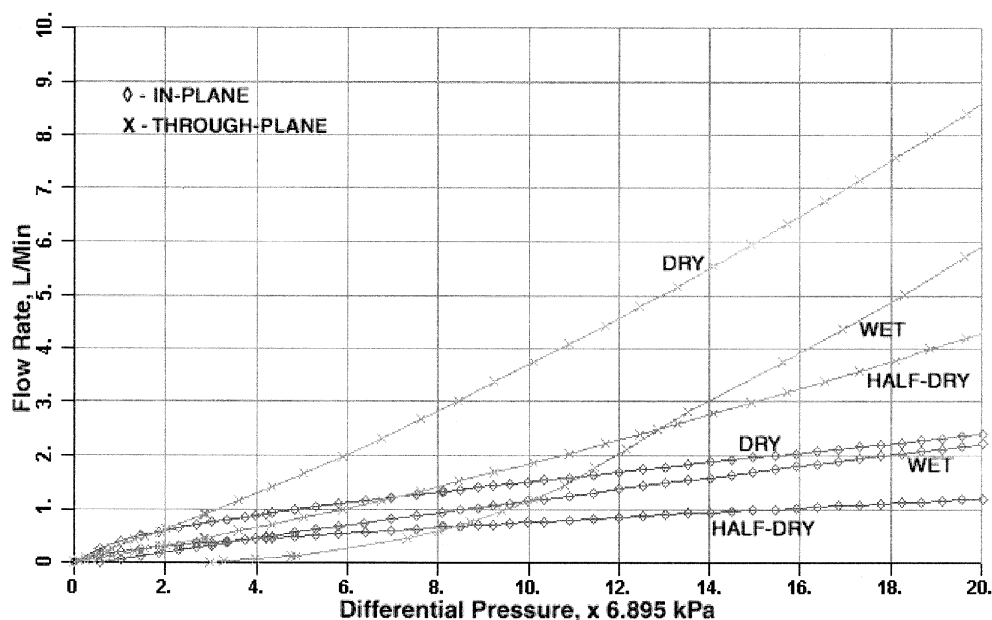


Fig. 7. Variation of flow rate with differential pressure for through-plane and in-plane flow.

Table 1  
Pore diameters in the two layers of the composite battery material

Layer no.	The largest pore diameter (μm)	The mean flow pore diameter (μm)	Technique
1	2.214	0.514	Through-plane
2	11.57	1.72	In-plane

is determined by its largest pore diameter. Any flaw present in the separator may also show up as the largest pore diameter.

The intersection of the wet curve and the half-dry curve gives the mean flow pressure which is converted to mean flow pore diameter. Half of the flow through the sample is through pores larger than the mean flow pore diameter. The mean flow pore diameters are listed in Table 1. Mean flow pore diameter is a measure of the permeability of fluids through the material [2].

3.3. Pore size distribution

The flow rate through a material is a function of pressure, properties of the gas and properties of the sample. For viscous flow the variable, pressure, can be separated from other variables [3]. We assume that flow rate can be expressed as the product of two functions such that one of these functions depends on pressure only and the other function is independent of pressure. The ratio of flow rates through the wet and the dry samples at the same pressure does not depend upon pressure. If  $F_w$  and  $F_d$  are flow rates through wet and dry samples respectively at the same pressure  $p_i$ ,  $\left(\frac{F_w}{F_d}\right)_{p_i}$  is independent of pressure. The cumu-

lative filter flow percent,  $(100 \times (F_w/F_d))$  obtained from Fig. 7 is shown in Fig. 8. The pores in layer no. 2 that are larger than those in layer no. 1 and are in the range of about 2–11.5 μm are responsible for almost 50% of flow (Fig. 8). Other differences between the layers are brought out by the pore size distribution.

The pore size distribution function,  $f$  is defined as:

$$f = - \frac{d[100 \times (F_w/F_d)]}{dD} \tag{10}$$

The leading negative sign on the right hand side of this Eq. is due to the fact that increase in pore diameter decreases the flow rate. The distribution functions were calculated from data in Fig. 7 and are shown in Fig. 9. The area under the distribution curve in a given pore diameter range yields percentage of flow through pores in that size range.

The through-plane test shows a group of small pores in the range of about 0.2–1.5 μm, while the in-plane test shows a group of small pores in the same range and a group of large pores over a wide range of about 2–11.5 μm. The small group of pores obtained from the through-plane test is in layer no. 1. The group of large pores found in the in-plane test is in layer no. 2. The group of small pores found in the in-plane test could be in both layers or in one of the layers. This small group of pores appears in a size range which is almost identical with that in layer no. 1. Therefore, the small group of pores found in the in-plane test is expected to be of layer no. 1. The pores in both layers are identified.

In the material investigated, the flow rates through the two groups of large and small pores are comparable. In many other composites the flow through the large pores dominates the in-plane flow. In such cases, determination of pore structures of the two layers by this technique becomes even easier.

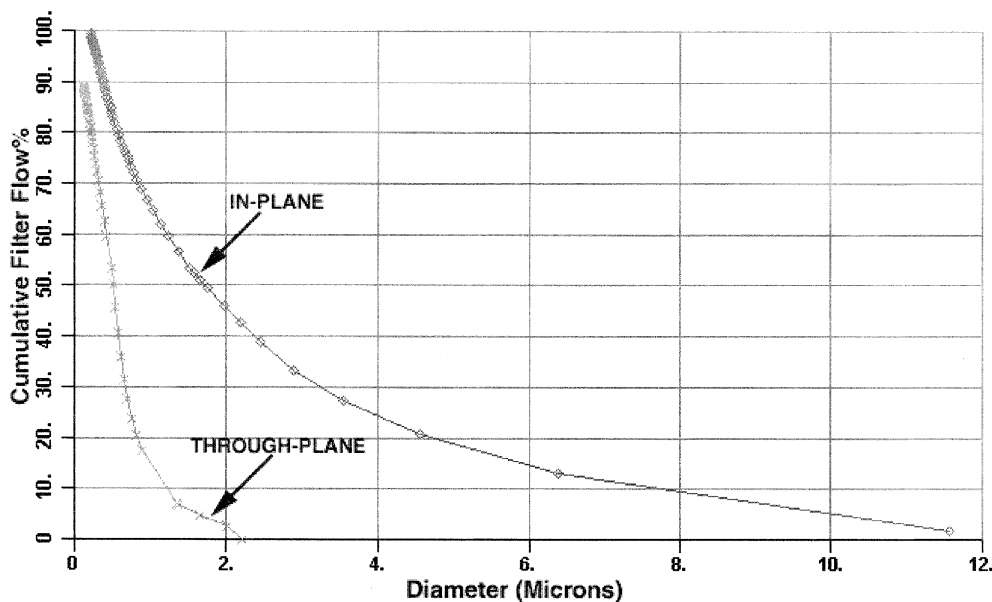


Fig. 8. Cumulative filter flow.

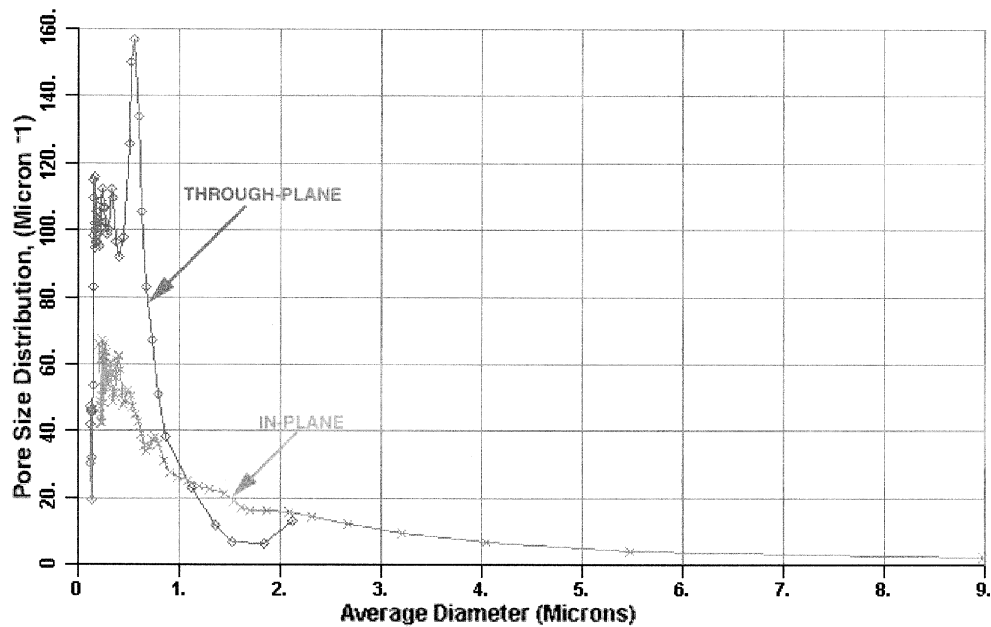


Fig. 9. Pore size distribution.

#### 4. Conclusions

1. The technique for measurement of change of flow rate with increase in differential pressure in the  $x$  and  $y$  directions and the  $z$  direction of a sheet material was described.
2. Flow through a composite sheet material for battery consisting of one of the electrodes and the separator in two layers was measured in the in-plane ( $x$  and  $y$  directions) and the through-plane ( $z$  direction).
3. The measurements yielded the largest pore diameter, the mean flow pore diameter, cumulative flow percent and pore size distribution.
4. For layer no. 1, the largest pore diameter was  $2.214\ \mu\text{m}$ ,

the mean flow pore diameter was  $0.514\ \mu\text{m}$  and the pores were in the range of about  $0.2\text{--}1.5\ \mu\text{m}$ . For layer no. 2, the largest pore diameter was  $11.57\ \mu\text{m}$ , the mean flow pore diameter was  $1.72\ \mu\text{m}$  and the pores were in the range of about  $2\text{--}11.5\ \mu\text{m}$ .

5. The pore structure of the two layers of the composite could be easily determined.

#### References

- [1] V. Gupta, A.K. Jena, *Adv. filtr. Sep. Technol.* 13b (1999) 833.
- [2] E. Mayer, *Fluid/Particle Sep. J.* 10 (2) (1997) 81.
- [3] C.R. Scheidegger, *The Physics of Flow Through Porous Media*, Macmillan, New York, 1957.